A Novel *V/f* Control of Induction Motors for Wide and Precise Speed Operation

Mineo Tsuji*, Shuo Chen**, Shin-ichi Hamasaki*

Xiaodan Zhao*, and Eiji Yamada*

* Department of Electrical and Electronic Engineering, Nagasaki University, Bunkyo-machi 1-14, Nagasaki 852-8521, (JAPAN)

** The College of Mechanical Engineering, Fuzhou University, Gong-ye Road 523, Fuzhou, (CHINA)

***Abstract*—The V/f control method is one of speed control methods for induction motors. We have proposed an auto-boost voltage method to compensate the voltage drop of stator impedance and a slip frequency compensation method to decrease the speed error caused by the change of load. Stability of the proposed V/f control system is analyzed by root locus. Steady-state torque-speed characteristics and transient responses of proposed system are presented by experimental system. Compared with the constant V/f control method, speed accuracy of proposed method is improved in various speeds and loads.**

***Index Terms*— Constant *V/f* control, auto-boost voltage, slip frequency compensation, induction motor.**

I. INTRODUCTION

The *V/f* control method is one of variable-speed control methods for induction motors (IM). Unfortunately, the motor performance deteriorates at low frequencies when the airgap flux decreases, because of the voltage drop across the stator leakage impedance. In addition, a rotor slip of IM is requisite for producing torque. This slip causes the error between the actual and desired speeds, and cannot be ignored in many cases. Therefore, some common problems have appeared as the applications of *V/f* control method for general-purpose inverters. One problem is that the starting torque is limited. Another is that the speed control accuracy becomes worse with load increase or frequency decrease. On the other hand, speed sensorless vector control of IM allows high performance control of speed and torque. But the application of speed sensorless vector control has also some problems. One problem is the system stability under the influence of parameter variation. Another is that the control system is relatively complicated. For general application of variable-speed drive system, the *V/f* control method is also attractive if the drive system does not need a fast dynamic response. The study on *V/f* control has been reported to improve the performance [1], [2].

To realize an advanced *V/f* control, we propose an auto-boost voltage method to compensate the voltage drop across the stator leakage impedance and a slip frequency compensation method to decrease the speed error[3]. By detecting stator currents, the voltage drop across the stator leakage impedance can be instantly calculated and added to the voltage command automatically when the load varies. The slip frequency related the load variation can be also calculated by the detected currents and added to the supply frequency command to compensate the motor speed reduction caused by the necessary torque producing slip. For stabilizing the system, two first-order lags are introduced in the feedback loops of voltage drop and slip frequency compensators. A linear model of the proposed system at a steady-state operation is derived and the system stability is analyzed in various speeds and loads. Experimental results of the proposed compensation method are presented. Compared with the constant V/f method, the speed accuracy is remarkably improved by the proposed method in various speeds and loads. The effectiveness of the proposed system has been verified by simulation and experimentation.

II. PROPOSED METHOD

A. Compensation of Stator Leakage Impedance

Fig.1 shows the steady-state equivalent circuit of induction motor. From Fig.1, Fig.2 shows a phasor diagram defined by a *d-q* reference frame with respect to V_s . According to the principle of constant vector control, E_0 in Fig. 1 must be proportional to the supply frequency for keeping rotor flux constant. Generally, E_0 is considered to be approximately equal to the input voltage V_s at high frequencies because V_s is greater than the voltage drop across the stator leakage impedance.

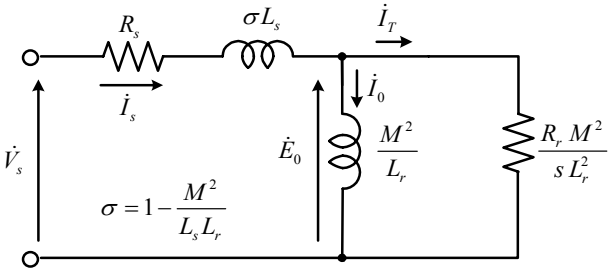

Fig. 1. Equivalent circuit of induction motor

978-1-4244-1663-9/08/$25.00 ©2008 IEEE

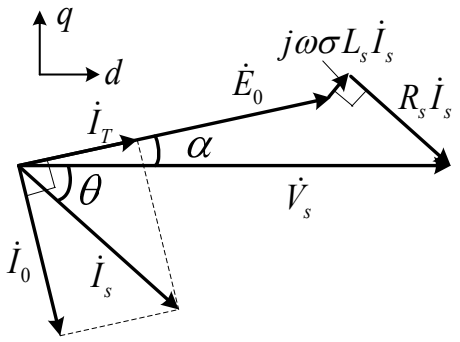

Fig. 2. Phasor diagram and definition of *d-q* reference frame.

But it is not valid at low frequencies or with heavy load, because this voltage drop becomes greater relatively and can not be ignored. Therefore, the influence of voltage drop must be considered. The *d-q* currents can be written as follows:

$$\begin{bmatrix} i_{sd} \\ i_{sq} \end{bmatrix} = \sqrt{2}\begin{bmatrix} \sin(\theta^* - \frac{\pi}{6}) & -\cos\theta^* \\ \cos(\theta^* - \frac{\pi}{6}) & \sin\theta^* \end{bmatrix}\begin{bmatrix} i_{sa} \\ i_{sb} \end{bmatrix} = \sqrt{3}I_s\begin{bmatrix} \cos\theta \\ -\sin\theta \end{bmatrix} \quad (1)$$

where θ is phase difference between the phase voltage and the phase current. Defining $X_s = \omega\sigma L_s$, the following equations can be obtained from Fig. 2.

$$V_s = E_0\cos\alpha + \frac{1}{\sqrt{3}}\left(R_s i_{sd} - X_s i_{sq}\right) \quad (2)$$

$$\sin\alpha = -\frac{1}{\sqrt{3}E_0}\left(X_s i_{sd} + R_s i_{sq}\right) \quad (3)$$

E_0 is proportional to the supply frequency. The magnitude of the auto-boost voltage can be calculated by

$$V_b^{'} = V_s - E_0 \quad (4)$$

Because of the inherently positive feedback characteristic of the auto-boost voltage, it is necessary to stabilize the system by introducing a first-lag in the feedback loop [2]. The actual auto-boost voltage command is obtained by

$$V_b = \frac{1}{1+\tau p}V_b^{'} \quad (5)$$

The phase voltage command is given by

$$V_s^* = E_0 + V_b \quad (6)$$

B. Compensation of Slip Frequency

This slip causes an error between the actual and desired speeds, and cannot be ignored in many cases, for example, at low frequency operation or at the heavy load operation.

From Fig. 1, the magnetizing current I_0 and the torque current I_T are obtained as follows:

$$I_0 = \frac{L_r E_0}{\omega M^2} \quad (7)$$

$$I_T = \frac{sE_0 L_r^2}{R_r M^2} \quad (8)$$

From (7) and (8), the slip frequency $f_{sl}^{'}$ is obtained by

$$f_{sl}^{'} = \frac{R_r}{2\pi L_r}\frac{I_T}{I_0} \quad (9)$$

I_0 and I_T shown in Fig. 2 are expressed as

$$\begin{bmatrix} I_0 \\ I_T \end{bmatrix} = \frac{1}{\sqrt{3}}\begin{bmatrix} \sin\alpha & -\cos\alpha \\ \cos\alpha & \sin\alpha \end{bmatrix}\begin{bmatrix} i_{sd} \\ i_{sq} \end{bmatrix} \quad (10)$$

In order to stabilize the system, a first-lag in the feedback loop is introduced as follow:

$$f_{sl} = \frac{1}{1+\tau p}f_{sl}^{'} \quad (11)$$

The actual supply frequency f^{**} can be calculated by

$$f^{**} = f^* + f_{sl} \quad (12)$$

where f^* is the frequency corresponding to speed command.

Fig. 3 shows the block diagram of proposed system. The output voltage error of PWM inverter caused by dead-time and voltage drop of IGBT is considered and the voltage commands are well pre-processed with a compensating algorithm [4].

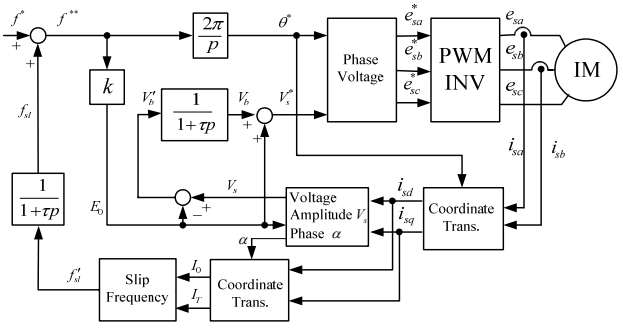

Fig. 3. Block diagram of proposed method.

III. Stability Analysis

Stability analysis of the proposed system shown in Fig. 3 is presented. By taking a small perturbation at a steady-state operating point, a linear model can be deduced. In order to analyze the IM, the *d-q* reference frame shown in Fig. 2 that rotates synchronously with the supply angle θ^* is chosen. By using the model of IM and the equations of controller, a linear model of the proposed system shown in Fig. 3 is derived as follows:

$$p\Delta\boldsymbol{x} = \boldsymbol{A}\Delta\boldsymbol{x} + \boldsymbol{B}\Delta\boldsymbol{r} \quad (13)$$

where, $\Delta\boldsymbol{x} = \left[\Delta i_{sd}, \Delta i_{sq}, \Delta\psi_{rd}, \Delta\psi_{rq}, \Delta\omega_r, \Delta V_b^*, \Delta f_{sl}^*\right]^T$

$$\Delta \boldsymbol{r} = \left[\Delta f^*, \Delta T_L \right]^T$$

$$\boldsymbol{A} = \begin{bmatrix} -a_1 & \omega & \frac{M}{\tau_r \sigma L_s L_r} & \frac{M\omega_r}{\sigma L_s L_r} & \frac{M\psi_{rq}}{\sigma L_s L_r} & \frac{\sqrt{3}}{\sigma L_s} & 2\pi i_{sq} + \frac{\sqrt{3}k}{\sigma L_s} \\ -\omega & -a_1 & -\frac{M\omega_r}{\sigma L_s L_r} & \frac{M}{\tau_r \sigma L_s L_r} & -\frac{M\psi_{rd}}{\sigma L_s L_r} & 0 & -2\pi i_{sd} \\ \frac{M}{\tau_r} & 0 & -\frac{1}{\tau_r} & \omega - \omega_r & -\psi_{rq} & 0 & 2\pi\psi_{rq} \\ 0 & \frac{M}{\tau_r} & \omega_r - \omega & -\frac{1}{\tau_r} & \psi_{rd} & 0 & -2\pi\psi_{rd} \\ -a_2\psi_{rq} & a_2\psi_{rd} & a_2 i_{sq} & -a_2 i_{sd} & 0 & 0 & 0 \\ a_3 & a_4 & 0 & 0 & 0 & -\frac{1}{\tau} & a_5 \\ a_8 & a_9 & 0 & 0 & 0 & 0 & -\frac{a_6 a_7 R_s i_{sq}}{f^{**2}} - \frac{1}{\tau} \end{bmatrix}$$

$$a_1 = \frac{1}{\sigma L_s}\left(R_s + \frac{M^2}{L_r \tau_r} \right) \ , \ a_2 = \frac{P^2 M}{4JL_r} \ ,$$

$$a_3 = \frac{1}{\sqrt{3}\tau}\left(R_s + \frac{X_s \sin\alpha}{\cos\alpha} \right) \ ,$$

$$a_4 = \frac{1}{\sqrt{3}\tau}\left(\frac{R_s \sin\alpha}{\cos\alpha} - X_s \right) \ ,$$

$$a_5 = \frac{k\left(\cos\alpha - 1\right)}{\tau} - \left(2\pi\sigma L_s + \frac{R_s \sin\alpha}{f^{**}\cos\alpha} \right) \frac{i_{sq}}{\sqrt{3}\tau} \ ,$$

$$a_6 = \frac{R_r}{2\pi L_r \tau} \ , \quad a_7 = \frac{I_0^2 + I_T^2}{\sqrt{3}\, k\, I_0^2 \cos\alpha}$$

$$a_8 = a_6\left(a_7\, 2\pi\sigma L_s - \frac{i_{sq}}{3I_0^2} \right) \ , \quad a_9 = a_6\left(a_7 \frac{R_s}{f^{**}} + \frac{i_{sd}}{3I_0^2} \right)$$

$$\sigma = 1 - \frac{M^2}{L_s L_r} \ , \ \tau_r = \frac{L_r}{R_r} \ , \ \omega = 2\pi f^{**}$$

The input variables are f^* corresponding to speed command N_r^* and the load torque T_L.

The loci of the poles calculated from $\boldsymbol{A}$ of (13) are shown in Figs. 4~7 at various speeds. The time constant τ of the first-lag is changed from 0.002 to 2.0 at the rated torque (8 Nm).

Figs. 4, 5, 6 and 7 show the root loci in which motor speeds are 30 rpm, 60 rpm, 1000 rpm and 1500 rpm respectively. The system becomes unstable if the time constant τ is very small. Giving consideration to all operation points located in a stable region, τ is selected as 1.0 for motoring mode in this paper.

Figs. 8 ~ 10 show the root loci of the poles in which the motor speeds are 30 rpm, 60 rpm and 90 rpm respectively. The load torque is changed from 0 Nm to 8 Nm. Fig. 11 shows the root locus in which the motor speeds are 300 rpm, 1000 rpm and 1500 rpm. From Figs. 8 ~ 11, the system is stable for all operating points. In particular, all of the poles shown in Fig.8 are in the stable region, though the poles are near to the imaginary axis along with increase of the load torque. The system performance is mainly influenced by the poles near imaginary axis.

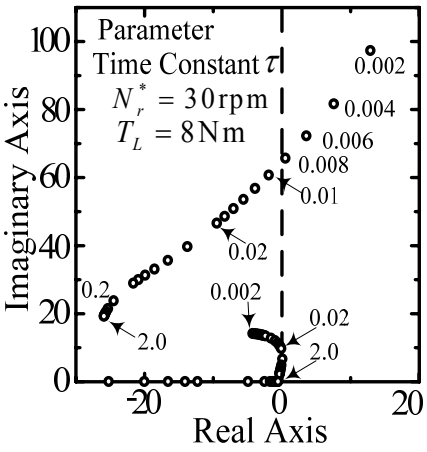

Fig. 4. Root loci with parameter τ at 30 rpm.

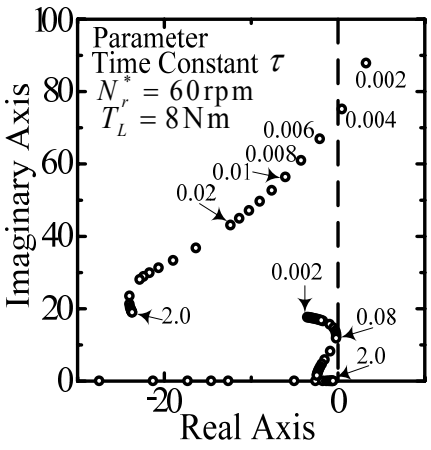

Fig. 5. Root loci with parameter τ at 60 rpm.

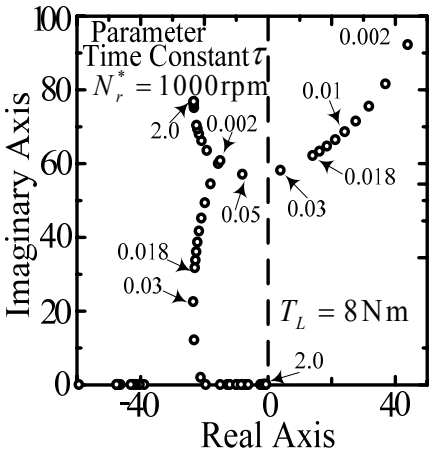

Fig. 6. Root loci with parameter τ at 1000rpm.

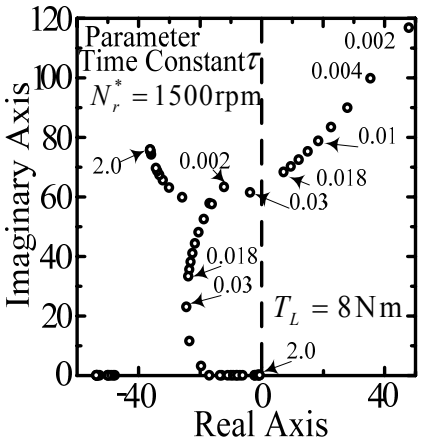

Fig. 7. Root loci with parameter τ at 1500 rpm.

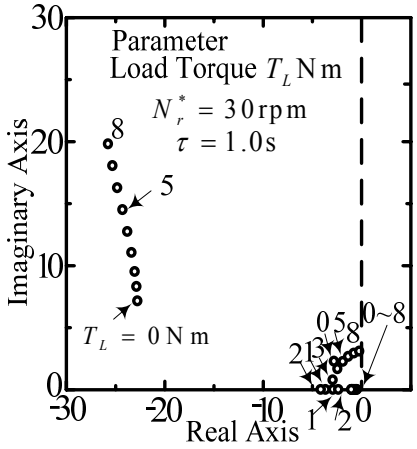

Fig. 8. Root loci with parameter T_L at 30 rpm.

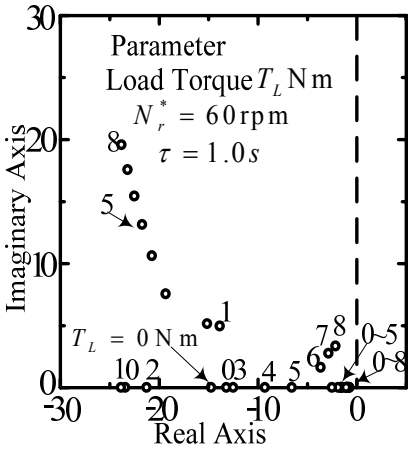

Fig. 9. Root loci with parameter T_L at 60 rpm.

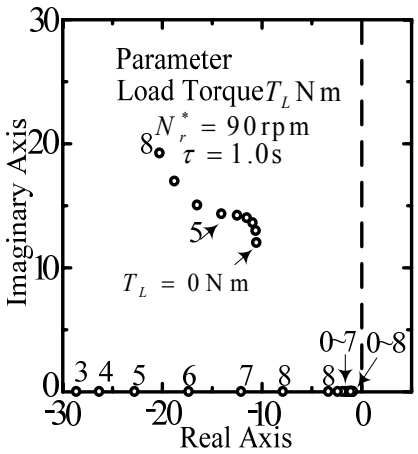

Fig. 10. Root loci with parameter T_L at 90 rpm.

IV. Experimental Results

A. Experimental System

The experimental system is shown in Fig. 12. The proposed control system was implemented by a DSP (TMS320C6713-225MHz) based PWM inverter. The sampling period is 200 μs. Because the dead time and the non-ideal features of IGBT influence the output voltage of the inverter, a compensating algorithm was applied to the experimental system [4]. In the following analysis, the tested induction machine has the nominal values shown in Table I. The rated torque is 8 Nm.

B. Experimental Results

Figs. 13 ~ 18 show the experimental results of the actual motor speed N_r, the auto-boost voltage V_b and the slip frequency f_{sl} when the load torque is changed.

Figs. 13 and 14 show the steady-state characteristics at speed command 30 rpm and 60 rpm respectively by proposed method. The rotor speed is controlled to its speed command. In these cases, the speed control cannot be realized by a simple constant V/f method without auto-boost voltage compensation. Figs. 15 ~ 18 show the

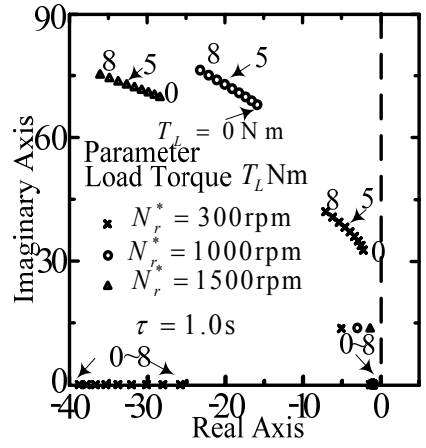

Fig. 11. Root loci with parameter T_L at 300, 1000, 1500rpm.

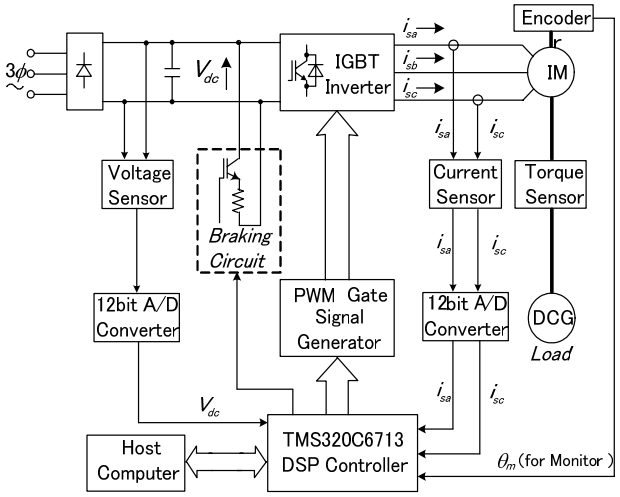

Fig. 12. Schematic of control system.

TABLE I
MEASURED DATA OF TESTED INDUCTION MOTOR

Stator resistance R_s [Ω]	1.6
Rotor resistance R_r [Ω]	0.85
Stator inductance L_s [H]	0.1176
Rotor inductance L_r [H]	0.1179
Mutual inductance M [H]	0.112

steady-state characteristics at 90 rpm, 300 rpm, 1000 rpm and 1500 rpm respectively by comparing the proposed method with the constant V/f method. Since the proposed method includes the auto-boost voltage and the slip frequency compensation, the steady-state error becomes smaller than the constant V/f method and the speed control is still realized when the load is applied to 8 Nm. The above experimental results show the effectiveness of the proposed method. Even at low frequency operation, the speed control is realized under heavy load condition.

Figs. 19 ~ 22 show the transient responses of the actual speed and the phase current under the load torque (4 Nm) for the step change of speed command. In Figs. 19 and 20, the speed command is changed from 30rpm to 90rpm. and from 200rpm to 300rpm respectively. Experimental result of the constant V/f method cannot be obtained in these operating points. Figs. 21 and 22 shows the transient response when the speed command is changed from 900rpm to 1000rpm and from 1400rpm to 1500rpm respectively. In Figs. 21 and 22, the upper wave is the results of the constant V/f method and the lower wave is those of the proposed method. Compared with them, the actual speed by the proposed method is converged to the speed command. Thus, it is confirmed that the proposed method is valid.

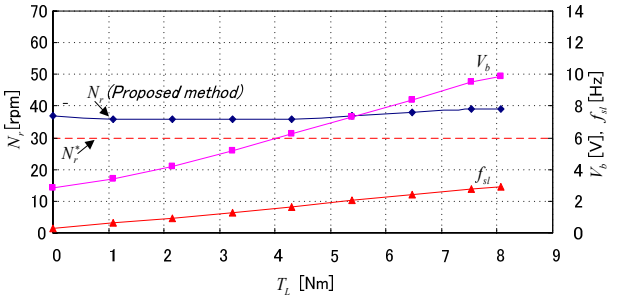

Fig. 13. Characteristics of load torque versus speed at 30 rpm.

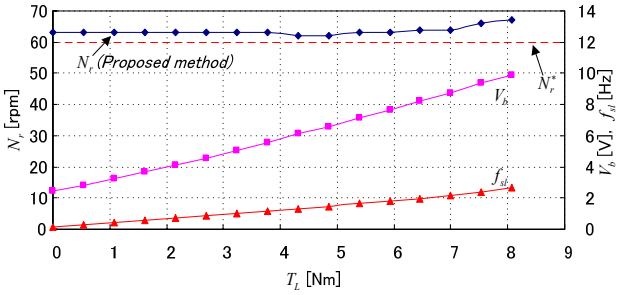

Fig. 14. Characteristics of load torque versus speed at 60 rpm.

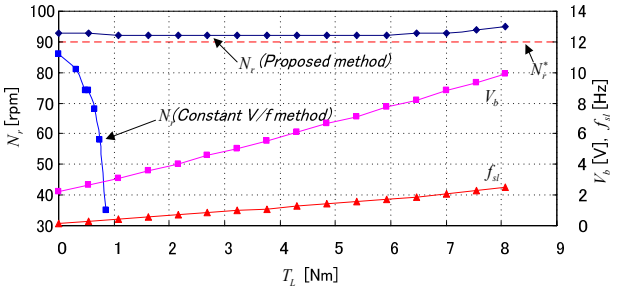

Fig. 15. Characteristics of load torque versus speed at 90 rpm.

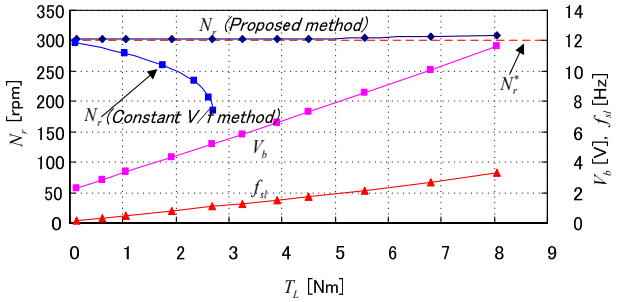

Fig. 16. Characteristics of load torque versus speed at 300 rpm.

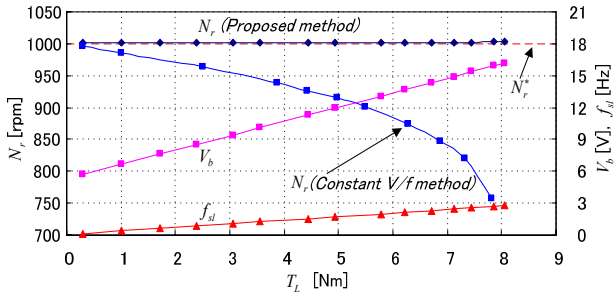

Fig. 17. Characteristics of load torque versus speed at 1000 rpm.

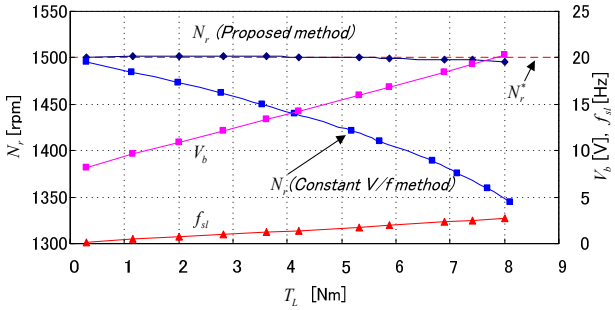

Fig. 18. Characteristics of load torque versus speed at 500rpm.

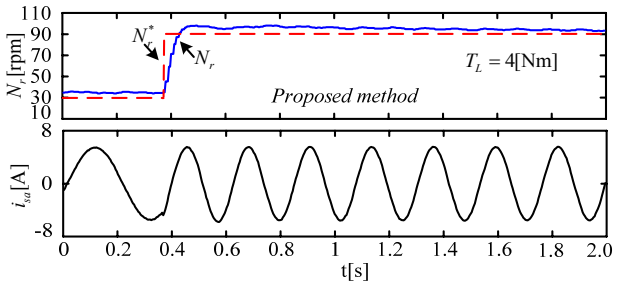

Fig. 19. Transient responses for step change of speed command from 30rpm to 90rpm.

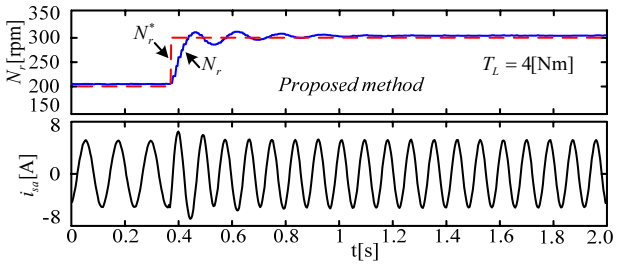

Fig. 20. Transient responses for step change of speed command from 200rpm to 300rpm.

V. Conclusions

A novel *V/f* control method has been presented. By calculating the *d-q* currents of IM, auto-boost voltage compensation for the voltage drop across stator leakage impedance and the slip frequency compensation are realized. The stability of the proposed system was discussed in detail and the time constant of the first-lag of these compensations was selected from viewpoint of system stability.

When the constant V/f method is used, the motor cannot be operated at very low speed. On the other hand, the proposed method can realize the speed control at very low frequency operation, such as 30 rpm, from no load to the rated load. Experimental results show that good speed control accuracy can be achieved by the proposed method. This method can be easily applied to existing *V/f* drives. Compared to sensorless vector control system, our method does not need any PI controllers for current control, speed control and speed estimation.

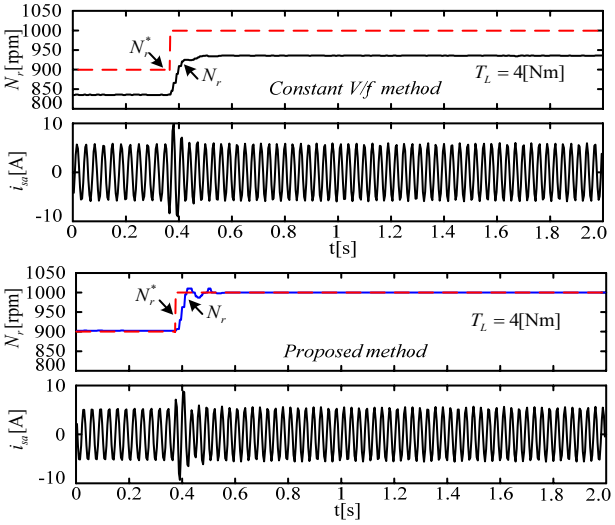

Fig. 21. Transient responses for step change of speed command from 900rpm to 1000rpm.

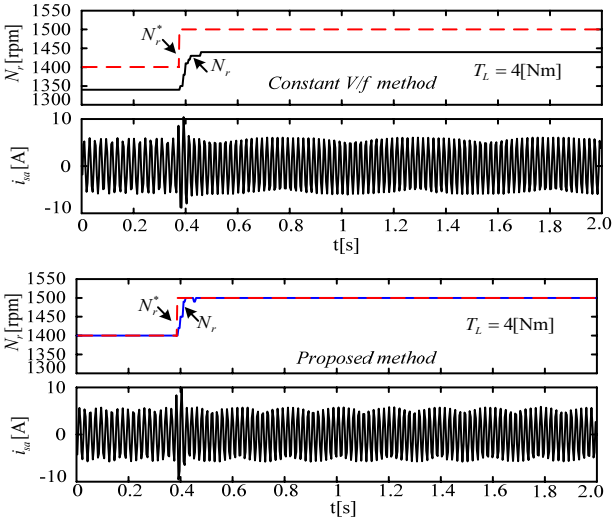

Fig. 22. Transient responses for step change of speed command from 1400 rpm to 1500 rpm.

References

[1] K. Koga, R. Ueda, and T. Sonoda, "Constitution of V/f control for reducing the steady state speed error to zero in induction motor drive systems", Conf. Rec. IEEE-IAS Annu. Meeting, pp. 639-646,1990.

[2] Alfredo M-G, Thomas A. Lipo, and Donald W. Novotny, "A new induction motor V/f control method capable of high-performance regulation at low speeds", *IEEE Trans. Ind. Appl., vol. 34, no. 4*, pp. 813–821, 1998.

[3] M. Tsuji, Y. Nakazaki, S. Chen and S. hamasaki: "Proposed method of new constant V/f control induction motor for general-purpose inverter" , *Proc. JIASC*, pp. 67-70, 2005

[4] M. Tsuji, S. Chen, K. Izumi and E. Yamada : "A sensorless vector control system for induction motors using *q*-axis flux with stator resistance identification", *IEEE Trans. Ind. Electronics*, Vol.48, No.1, pp.185-194, 2001.